HHS Public Access

Author manuscript

AJR Am J Roentgenol. Author manuscript; available in PMC 2019 March 28.

Published in final edited form as:

AJR Am J Roentgenol. 2019 January ; 212(1): 124–129. doi:10.2214/AJR.18.19742.

Multiparametric MRI Features and Pathologic Outcome of Wedge-Shaped Lesions in the Peripheral Zone on T2-Weighted Images of the Prostate

Aritrick Chatterjee[1], **Sevil Tokdemir**[2], **Alexander J. Gallan**[3], **Ambereen Yousuf**[1], **Tatjana Antic**[3], **Gregory S. Karczmar**[1], and **Aytekin Oto**[1]

[1]Department of Radiology, University of Chicago, 5841 S Maryland Ave, Chicago, IL 60637.

[2]Department of Radiology, Bezmialem Vakif University, Istanbul, Turkey.

[3]Department of Pathology, University of Chicago, Chicago, IL.

Abstract

OBJECTIVE.—This study investigates the multiparametric MRI (mpMRI) characteristics and pathologic outcome of wedge-shaped lesions observed on T2-weighted images.

MATERIALS AND METHODS.—Seventy-six patients with histologically confirmed prostate cancer underwent preoperative 3-T MRI before undergoing radical prostatectomy. Two radiologists worked in consensus to mark wedge-shaped regions of hypointensity on T2-weighted images and assess their appearance on apparent diffusion coefficient (ADC) maps (to determine the degree of hypointensity) and dynamic contrast-enhanced (DCE) MRI (DCE-MRI) (to assess whether they showed early enhancement). The pathologic outcome of wedge-shaped lesions was assessed by matching MR images with whole-mount histologic specimens retrospectively. The difference in quantitative ADC values between malignant and benign wedge-shaped lesions was assessed using a *t* test.

RESULTS.—Thirty-five wedge-shaped regions were identified, 12 (34%) of which were found be malignant. Most malignant wedge-shaped regions were highly hypointense (10/12; 83%) on ADC maps and showed early enhancement on DCE-MRI (7/12; 58%). However, benign wedge-shaped lesions were predominantly mildly hypointense (13/23; 57%) on ADC maps and showed no early enhancement (15/23; 65%). Histologic correlates of the benign wedge-shaped regions showed prostatitis (acute inflammation [7/23; 30%] or chronic inflammation [9/23; 39%]), hemosiderin-laden macrophages (6/23; 26%), prominent blood vessels (7/23; 30%), intraluminal blood (6/23; 26%), and nonspecific atrophy (6/23; 26%). The mean (± SD) quantitative ADC value of malignant wedge-shaped regions (1.13 ± 0.11 $\mu m^2/ms$) was significantly lower ($p = 0.0001$) than that of benign wedge-shaped regions (1.52 ± 0.27 $\mu m^2/ms$).

CONCLUSION.—This study shows that a greater percentage of wedge-shaped features are malignant than was previously thought. Of importance, mpMRI (specifically, ADC maps) can distinguish between malignant and benign wedge-shaped features.

Address correspondence to A. Oto (aoto@radiology.bsd.uchicago.edu).

Keywords

apparent diffusion coefficient; histology; prostate MRI; T2-weighted images; wedge-shaped lesions

Prostate rostate cancer is a major concern among men, with one of six men affected by the disease in their lifetime [1]. MRI is increasingly being used for prostate cancer diagnosis because of its advantage over traditional prostate-specific antigen (PSA) evaluation and transrectal ultrasound–guided biopsies, which is its ability to sample the whole prostate noninvasively [2–4]. MRI provides information not only about the presence of prostate cancer but also about the location, size, and aggressiveness of prostate cancer lesions [5, 6]. Despite the good soft-tissue contrast capability and higher sensitivity and negative predictive value of MRI for prostate cancer detection, a large number of prostate cancers go undetected [3, 7, 8]. In addition, benign features such as prostatitis, benign prostatic hyperplasia, atrophy, and other features can mimic prostate cancer on multiparametric MRI (mpMRI) [9–13].

Among the pitfalls of mpMRI in prostate cancer detection is the appearance of wedge-shaped regions of hypointensity on T2-weighted images. Until recently, no definitive morphologic criteria existed with which to differentiate between benign and malignant prostatic lesions. The Prostate Imaging Reporting and Data System (PI-RADS) [14] and the European Society of Urogenital Radiology [15] consensus guidelines assigned PI-RADS category 2 to wedge-shaped hypointense regions with indistinct margins noted in the peripheral zone on T2-weighted images. These regions are generally associated with prostatitis, atrophy, or fibrosis and therefore are assigned a low PI-RADS assessment category, which indicates that a low likelihood for a malignant lesion is associated with the wedge-shaped regions. These regions show only a mildly decreased apparent diffusion coefficient (ADC) value and possibly result in false-positive findings on dynamic contrast-enhanced (DCE) MRI (DCE-MRI). There have been similar suggestions that a wedge shape could be caused by changes related to inflammation or hemorrhage or could be a consequence of prostatitis [16–19]. In addition, a round, oval, or irregular shape with blurred borders is more suspicious for prostate cancer than are wedge-shaped regions.

However, to our knowledge, the study by Cruz et al. [20] is the only study that has examined the pathologic outcome of wedge-shaped regions, with only one of 27 wedge-shaped regions in 70 patients found to be malignant. However, the pathologic results were based on systematic 12-core needle biopsies of the whole prostate, and only T2-weighted imaging was used. The lack of correlation of findings from whole-mount histologic specimens and mpMRI in the earlier study and a clear lack of consensus among radiologists regarding the mpMRI features and pathologic outcome of wedge-shaped regions underscore the need for further research.

The present study investigates the mpMRI characteristics and pathologic outcome of wedge-shaped lesions on T2-weighted images. A better understanding of the pathologic outcomes of wedge-shaped lesions and their appearance on mpMRI, obtained by using a closer match

of whole-mount histologic specimens and MR images, will improve the performance of mpMRI in the diagnosis of prostate cancer.

Materials and Methods

This retrospective HIPAA-compliant study was conducted after approval was given by the institutional review board at the University of Chicago and prior informed patient consent was obtained.

Study Patients

All 76 patients with prior biopsy-proven prostate cancer who underwent preoperative MRI performed at our research center between February 2014 and August 2016 before subsequently undergoing radical prostatectomy were included in the study. Among the contraindications to inclusion in the study were prior receipt of radiation or hormonal replacement therapy (leading to alterations in the prostatic signal on MRI). The mean patient age was 59 years (range, 40–76 years), and the mean PSA level before MRI was 8.1 ng/mL (range, 0.8–66.1 ng/mL).

MRI

Patients underwent preoperative MRI performed using a 3-T system (Achieva MR, Philips Healthcare) with a six-channel cardiac phased-array coil placed around the pelvis and an endorectal coil (Medrad, Bayer HealthCare). A 1-mg dose of glucagon (Glucagon, Eli Lilly) was injected before MRI was performed, to limit peristalsis of the rectal wall. Multiparametric MR images of the prostate, including T2-weighted, DW, and DCE images, were obtained. The typical MRI parameters that were used are described in detail in Table 1.

Histologic Analysis

The patients subsequently underwent radical prostatectomy. The prostate was fixed in formalin and was serially sectioned (in 4-mm slices) approximately in the same plane shown in the MR images. Tissue submitted for analysis was embedded in paraffin and stained with H and E, whole-mount slides were made, and the slides were examined by two expert pathologists with 15 and 5 years of experience. Outlines of cancer were marked on the whole-mount slides.

MR Image Analysis

Multiparametric MR images for all 76 patients were loaded on a PCampReview custom module in an open-source software platform for medical image informatics, image processing, and 3D visualization (3D Slicer) [21]. Two radiologists with 15 and 3 years of experience in prostate MRI who were blinded to the pathologic results reviewed the T2-weighted images and drew ROIs on wedge-shaped areas of hypointensity on the T2-weighted images. Only one consensus ROI was drawn for every wedge-shaped lesion. The MR images from different mpMRI sequences were coregistered to T2-weighted images, and the ROIs were propagated to other mpMRI sequences.

ADC values were measured on a voxel-by-voxel basis with the use of DW images (with all b values), with use of the following monoexponential signal decay model:

$$S = S_0 \exp(-b \cdot ADC),$$

where S_0 is the maximum spin-echo signal without DW, S is the attenuated spin-echo signal with DW, and b (the b value) is the DW factor.

ADC maps and DCE-MR images were also reviewed by the same radiologists. ROIs marked on wedge-shaped regions were categorized as highly hypointense, mildly hypointense, or isointense on ADC maps and as showing either early enhancement or no early enhancement on early phase DCE-MR images. The DCE-MRI signal intensity curve over time was analyzed for these ROIs and was categorized as either type 1 (denoting progressive enhancement), type 2 (indicating a plateau), or type 3 (denoting wash-in and washout), similar to the categorization used in a previous study [22].

Pathologic Outcome

The wedge-shaped regions were matched with histologically confirmed prostate cancer on whole-mount sections on the basis of the consensus of the radiologists and pathologists. The slides were retrospectively reviewed to assess for the presence or absence of pathologic findings in the region of the prostatectomy corresponding to the wedge-shaped lesion seen on MRI. In particular, the slides were assessed for discrete pathologic lesions limited to the wedge-shaped region, rather than nonspecific pathologic findings that were also seen in other areas of the prostate, and would be unlikely to explain the wedge-shaped lesion seen on MRI.

Quantitative Multiparametric MRI and Statistical Analysis

Quantitative ADC values for all the ROIs drawn on wedge-shaped regions were measured using an in-house program written using a multiparadigm numerical computing environment and proprietary programming language (Matlab, version 2016b, MathWorks). A two-tailed *t* test was performed to find any statistical difference in mean ADC values between benign and malignant wedge-shaped regions, with the use of statistical software (SPSS, version 4, IBM). ROC analysis was performed to evaluate the performance of quantitative ADC values in distinguishing benign and malignant wedge-shaped features.

Results

A total of 35 wedge-shaped regions of hypointensity on T2-weighted images were identified by the radiologists. Of the 35 wedge-shaped regions, only 12 (34%) were found to be malignant lesions. Of the malignant wedge-shaped lesions, one lesion had a Gleason score of 3 + 3, seven had a Gleason score of 3 + 4, three had a Gleason score of 4 + 3, and one had a Gleason score of 4 + 5. A discrete histologic correlate was identified for 17 of the 23 benign wedge-shaped regions (74%). These pathologic findings, several of which were frequently seen within the same wedge-shaped region, included prostatitis (acute inflammation [7/23; 30%] and chronic inflammation [9/23; 39%]), intraluminal

hemosiderin-laden macrophages (6/23; 26%), intraluminal blood (6/23; 26%), and prominent intraparenchymal blood vessels (7/23; 30%). In six cases (26%), nonspecific atrophy was present, but no discrete histologic correlates were identified. None of the cases contained previously undiagnosed prostate cancer in the wedge-shaped regions. Figure 1 shows common histologic features found in benign wedge-shaped lesions and corresponding wedge-shaped regions on T2-weighted images.

Figure 2 shows representative examples of a malignant wedge-shaped lesion as seen on T2-weighted MRI and its appearance on mpMRI, ADC maps, and DCE-MRI. Similarly, examples of images of wedge-shaped lesions that were found to be benign are shown in Figure 3. The imaging characteristics of both benign and malignant wedge-shaped lesions on mpMRI are presented in Table 2.

Apparent Diffusion Coefficient Maps

Most malignant wedge-shaped regions were highly hypointense (10/12; 83%) on ADC maps. Only a small number of wedge-shaped malignant lesions were mildly hypointense (2/12; 17%), whereas none of the wedge-shaped features were isointense (17%; 0/12) with respect to surrounding benign tissue on ADC maps. However, the benign wedge-shaped lesions were predominantly mildly hypointense (13/23; 57%) on ADC maps. Other lesions were either highly hypointense (7/23; 30%) or isointense (3/23; 13%) on ADC maps.

Of importance, the mean (± SD) quantitative ADC value of malignant wedge-shaped regions (1.13 ± 0.11 $\mu m^2/ms$) was significantly lower ($t = 4.472$, $p = 0.0001$) than that of benign wedge-shaped regions (1.52 ± 0.27 $\mu m^2/ ms$). ROC analysis revealed an AUC value of 0.90 (95% CI, 0.79–1.00) ($p < 0.0001 \times 10^{-4}$) for differentiating between malignant and benign prostate tissue with the use of quantitate ADC values.

Dynamic Contrast-Enhanced MRI

The most common feature of malignant wedge-shaped features was early enhancement on DCE-MRI (7/12; 58%), which showed type 1 curve showing progressive signal enhancement over time (6/12; 50%). Five of 12 wedge-shaped malignant regions (42%) showed no early enhancement on DCE-MRI, whereas type 2 plateau (2/12; 17%) and type 3 wash-in and washout curve types (4/12; 33%) were seen in a small number of malignant wedge-shaped lesions.

Alternatively, most benign wedge-shaped lesions showed no early enhancement (15/23; 65%) and a type 2 curve (10/23; 43%). However, a small number of cases showed early enhancement (8/23; 35%) and type 1 (6/23; 26%) and type 3 (7/23; 30%) DCE-MRI curves.

Discussion

A greater percentage of wedge-shaped lesions were found to be malignant than has previously been shown in published literature [20]. However, pathologic outcomes in the previous literature were based on systematic 12-core needle biopsies of the whole prostate. The lack of whole-mount histologic correlates in the earlier study further highlights that

biopsies could potentially miss numerous cancers, compared with the reference standard of histologic analysis of prostatectomy specimens [3, 23, 24].

The PI-RADS version 2 guidelines use wedge-shaped hypointensity as part of the categorization scheme for peripheral zone abnormalities seen on T2-weighted images, and wedge-shaped hypointensities are assigned a score of 2 (a T2-weighted imaging score), which is suggestive of a benign lesion. These lesions are upgraded to PI-RADS category 3 if they are associated with a focal abnormality that is mildly to moderately hypointense on ADC maps (DWI score, 3). If they also show early enhancement on DCE or if they show focal abnormality that is markedly hypointense on ADC maps (DWI score, 4), then they are upgraded to PI-RADS category 4. Our results show that the shape of the lesion on T2-weighted imaging alone is not a good predictor of pathologic outcome. Our results are similar to those of a recent observational study that showed that lesion shape, including a wedge shape in the peripheral zone, is not effective in predicting significant cancer for PI-RADS category 4 lesions (positive predictive value, < 50%) [25].

A previous study by Cruz et al. [20] investigated wedge-shaped lesions using T2-weighted imaging only. Our results show that mpMRI is effective in predicting the pathologic outcome of wedge-shaped lesions, specifically with the use of quantitative ADC values. ADC values show high diagnostic accuracy in differentiating between malignant and benign wedge-shaped lesions because of the significant difference in the ADC values between them. However, early enhancement on DCE-MRI is not effective in the differentiation of malignant and benign wedge-shaped lesions. These results are in good agreement with PI-RADS recommendations [14] in which ADC maps derived from DWI are the primary sequence, whereas DCE-MRI is the secondary sequence for prostate cancer detection and PI-RADS categorization in the peripheral zone. In addition, the DCE-MRI curve type of the signal intensity over time was not useful in differentiating between benign and malignant wedge-shaped lesions. This result is similar to results from a previous study that found that curve type performs poorly in the differentiation of prostate cancer from healthy prostatic tissue [22].

Wedge-shaped lesions in the peripheral zone on T2-weighted images are assigned a PI-RADS category of 2, indicating a low likelihood for malignancy [14]. However, because a greater percentage of wedge-shaped features were found to be malignant, mpMRI findings and, specifically, quantitative ADC values should be used to predict the pathologic outcome of wedge-shaped lesions on T2-weighted images, with significantly lower quantitative ADC values associated with the presence of prostate cancer and therefore resulting in improved interpretation of prostate mpMRI. These results are in good agreement with the PI-RADS recommendations because DWI is the primary sequence used for determining the PI-RADS assessment category for lesions in the peripheral zone.

In addition, the previous study [20] did not access the pathologic outcome of the benign features. The wedge-shaped lesions are commonly attributed primarily to prostatitis [14]. Although prostatitis is the most common histologic correlate, other features, including intraluminal hemosiderin-laden macrophages, intraluminal blood, and prominent blood vessels, can also manifest as wedge-shaped lesions. Previous studies have shown that

prostatitis and atrophy appear hypointense on T2-weighted images [9, 17, 18, 26]. However, some cases showed only nonspecific atrophy that was not thought to explain the wedge-shaped regions. The susceptibility effects resulting from the presence of iron in hemosiderin-laden macrophages, prominent blood vessels, and intraluminal blood could potentially reduce the T2 relaxation time and reduce the in-phase signal intensity on T2-weighted images and therefore mimic prostate cancer [27, 28]. Whether the presence of intraluminal blood and hemosiderin-laden macrophages represents a pathologic process completely distinct from prostatitis is unclear. It is possible that acute and chronic inflammation as well as intraluminal blood and hemosiderin-laden macrophages are all related manifestations of single inflammatory insult, which would explain why several of these pathologic features were found within the same wedge-shaped lesion. However, the presence of prominent intraparenchymal blood vessels may represent a distinct pathologic lesion that simply shares MRI features with the previous histologic correlates.

The present study has a few limitations. Although the reason for the hypointensity on T2-weighted images could be explained for pathologic findings in these wedge-shaped lesions, the actual reason why they exhibit a specific shape is still unknown. In addition, we did not investigate other lesion shapes (i.e., oval, linear, lenticular, and other shapes) that can mimic prostate cancer on mpMRI. Similarly, only qualitative DCE-MRI was used, in accordance with original PI-RADS (focusing on curve type) and PI-RADS version 2 (focusing on early enhancement) guidelines. Several cases showed no definite histologic correlate, which may have resulted from an imprecise match between the radiologic and pathologic lesions, limitations of correlating 2D histologic sections with 3D space, or causes of wedge-shaped MRI lesions that are not discernable on histologic examination. Unenhanced T1-weighted images were not used in the analysis, which is another limitation of this study. It might be possible that some hypointense features on T2-weighted images were caused by prior biopsy and hemorrhage, and analysis of unenhanced T1-weighted images might be helpful in this respect. In addition, we expect to see bright T1 signal in hemosiderin-laden cases, which might add to improvement in differentiation between benign and malignant wedge-shaped lesions.

In conclusion, the present study shows that a greater percentage of wedge-shaped features are malignant than was previously thought. Benign conditions such as prostatitis (acute and chronic inflammation), hemosiderin-laden macrophages, prominent blood vessels, intraluminal blood, and atrophy can create a wedge-shaped region on T2-weighted-MRI. Of importance, mpMRI (specifically, the ADC value) can distinguish between malignant and benign wedge-shaped features. Therefore, the radiologist should consult quantitative ADC values to interpret the pathologic outcome of wedge-shaped lesions.

Acknowledgments

A. Oto received research grants from Koninklijke Philips Healthcare and Guerbet, is on the medical advisory board of Profound Medical, Inc., and is a speaker for Bracco.

Supported by Philips Healthcare and grants NIH R01 CA172801 and NIH 1S10OD018448–01 from the National Institutes of Health.

References

1. Siegel RL, Miller KD, Jemal A. Cancer statistics, 2016. CA Cancer J Clin 2016; 66:7–30 [PubMed: 26742998]
2. Litwin MS, Tan H. The diagnosis and treatment of prostate cancer: a review. JAMA 2017; 317:2532–2542 [PubMed: 28655021]
3. Ahmed HU, El-Shater Bosaily A, Brown LC, et al. Diagnostic accuracy of multi-parametric MRI and TRUS biopsy in prostate cancer (PROMIS): a paired validating confirmatory study. Lancet 2017; 389:815–822 [PubMed: 28110982]
4. Panebianco V, Barchetti F, Sciarra A, et al. Multiparametric magnetic resonance imaging vs. standard care in men being evaluated for prostate cancer: a randomized study. Urol Oncol 2015; 33:17.e1–17.e7
5. Woo S, Suh CH, Kim SY, Cho JY, Kim SH. Diagnostic performance of Prostate Imaging Reporting and Data System version 2 for detection of prostate cancer: a systematic review and diagnostic meta-analysis. Eur Urol 2017; 72:177–188 [PubMed: 28196723]
6. Isebaert S, Van den Bergh L, Haustermans K, et al. Multiparametric MRI for prostate cancer localization in correlation to whole-mount histopathology. J Magn Reson Imaging 2013; 37:1392–1401 [PubMed: 23172614]
7. Moldovan PC, Van den Broeck T, Sylvester R, et al. What is the negative predictive value of multiparametric magnetic resonance imaging in excluding prostate cancer at biopsy? A systematic review and meta-analysis from the European Association of Urology Prostate Cancer Guidelines Panel. Eur Urol 2017; 72:250–266 [PubMed: 28336078]
8. Hansen NL, Barrett T, Kesch C, et al. Multicentre evaluation of magnetic resonance imaging supported transperineal prostate biopsy in biopsy-naïve men with suspicion of prostate cancer. BJU Int 2018; 122:40–49 [PubMed: 29024425]
9. Kitzing YX, Prando A, Varol C, Karczmar GS, Maclean F, Oto A. Benign conditions that mimic prostate carcinoma: MR imaging features with histopathologic correlation. RadioGraphics 2016; 36:162–175 [PubMed: 26587887]
10. Lovett K, Rifkin MD, McCue PA, Choi H. MR imaging characteristics of noncancerous lesions of the prostate. J Magn Reson Imaging 1992; 2:35–39 [PubMed: 1377976]
11. Quint LE, Van Erp JS, Bland PH, et al. Prostate cancer: correlation of MR images with tissue optical density at pathologic examination. Radiology 1991; 179:837–842 [PubMed: 2028002]
12. Schiebler ML, Tomaszewski JE, Bezzi M, et al. Prostatic carcinoma and benign prostatic hyperplasia: correlation of high-resolution MR and histopathologic findings. Radiology 1989; 172:131–137 [PubMed: 2472644]
13. Schiebler ML, Schnall MD, Pollack HM, et al. Current role of MR imaging in the staging of adenocarcinoma of the prostate. Radiology 1993; 189:339–352 [PubMed: 8210358]
14. Weinreb JC, Barentsz JO, Choyke PL, et al. PI-RADS Prostate Imaging – Reporting and Data System: 2015, version 2. Eur Urol 2016; 69:16–40 [PubMed: 26427566]
15. Barentsz JO, Richenberg J, Clements R, et al. ESUR prostate MR guidelines 2012. Eur Radiol 2012; 22:746–757 [PubMed: 22322308]
16. Margolis DJ. Multiparametric MRI for localized prostate cancer: lesion detection and staging. BioMed Res Int 2014; 2014:684127 [PubMed: 25525600]
17. Sah VK, Wang L, Min X, et al. Multiparametric MR imaging in diagnosis of chronic prostatitis and its differentiation from prostate cancer. Radiology of Infectious Diseases 2015; 1:70–77
18. Szolar DH, Ranner G, Preidler KW, Lax S. Non-granulomatous prostatitis: MRI image with endorectal surface coil (“endo-MRI”). Aktuelle Radiol 1995; 5:67–69 [PubMed: 7888435]
19. White S, Hricak H, Forstner R, et al. Prostate cancer: effect of postbiopsy hemorrhage on interpretation of MR images. Radiology 1995; 195:385–390 [PubMed: 7724756]
20. Cruz M, Tsuda K, Narumi Y, et al. Characterization of low-intensity lesions in the peripheral zone of prostate on pre-biopsy endorectal coil MR imaging. Eur Radiol 2002; 12:357–365 [PubMed: 11870434]

21. Chatterjee A, He D, Fan X, et al. Performance of ultrafast DCE-MRI for diagnosis of prostate cancer. Acad Radiol 2017; 25:349–358 [PubMed: 29167070]
22. Hansford BG, Peng Y, Jiang Y, et al. Dynamic contrast-enhanced MR imaging curve-type analysis: is it helpful in the differentiation of prostate cancer from healthy peripheral zone? Radiology 2015; 275:448–457 [PubMed: 25559231]
23. Bak JB, Landas SK, Haas GP. Characterization of prostate cancer missed by sextant biopsy. Clin Prostate Cancer 2003; 2:115–118 [PubMed: 15040873]
24. Serefoglu EC, Altinova S, Ugras NS, Akincioglu E, Asil E, Balbay MD. How reliable is 12-core prostate biopsy procedure in the detection of prostate cancer? Can Urol Assoc J 2013; 7:E293–E298 [PubMed: 22398204]
25. Shankar PR, Curci NE, Davenport MS. Characteristics of PI-RADS 4 lesions within the prostatic peripheral zone: a retrospective diagnostic accuracy study evaluating 170 lesions. Abdom Radiol (NY) 2018; 43:2176–2182 [PubMed: 29198006]
26. Panebianco V, Barchetti F, Barentsz J, et al. Pitfalls in interpreting mp-MRI of the prostate: a pictorial review with pathologic correlation. Insights Imaging 2015; 6:611–630 [PubMed: 26385690]
27. Barbosa JHO, Santos AC, Salmon CEG. Susceptibility weighted imaging: differentiating between calcification and hemosiderin. Radiol Bras 2015; 48:93–100 [PubMed: 25987750]
28. Leftin A, Zhao H, Turkekul M, de Stanchina E, Manova K, Koutcher JA. Iron deposition is associated with differential macrophage infiltration and therapeutic response to iron chelation in prostate cancer. Sci Rep 2017; 7:11632 [PubMed: 28912459]

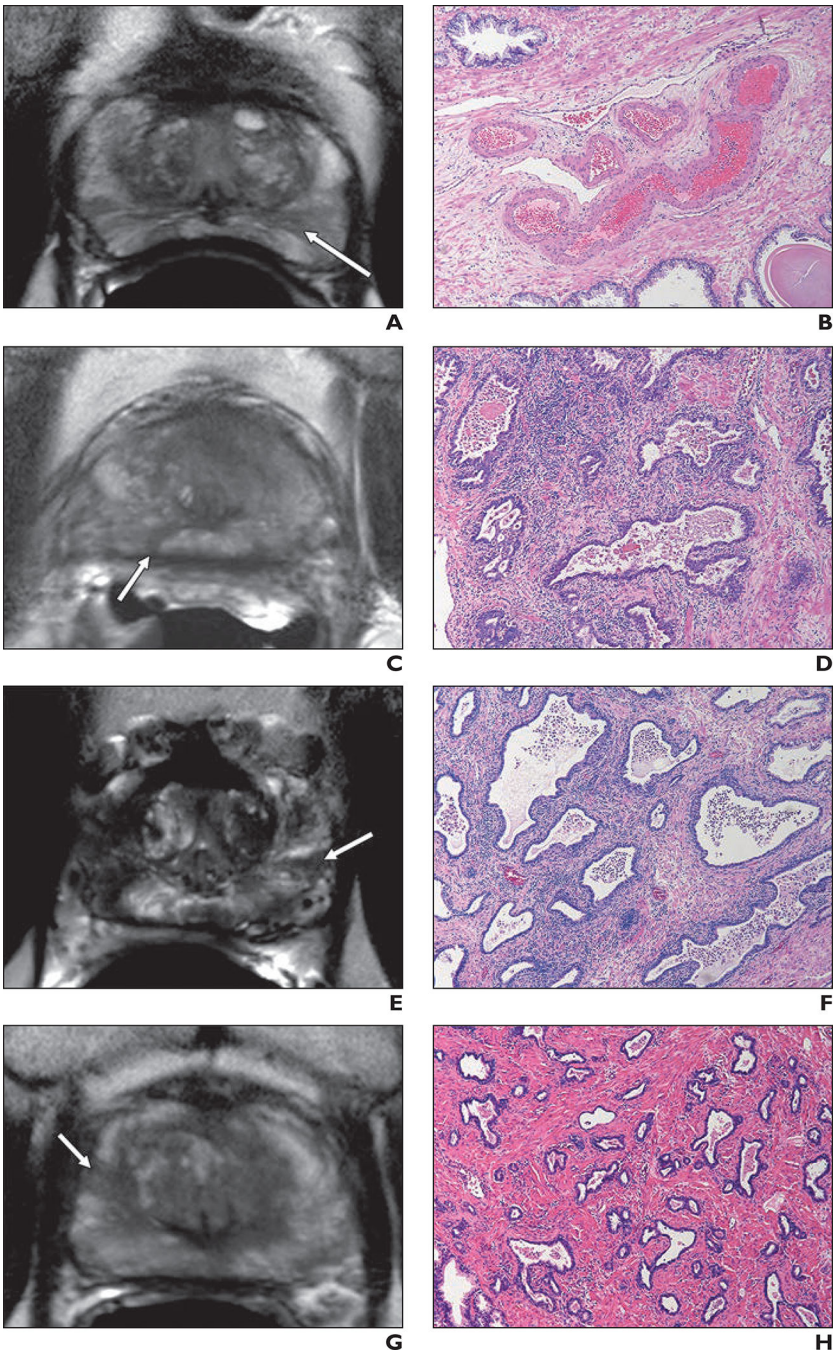

Fig. 1—.

Common histologic features of benign wedge-shaped prostate lesions.

A and **B,** 66-year-old man with prostate cancer. T2-weighted MR image (**A**) and corresponding photomicrograph (H and E, ×10) (**B**) show prominent intraparenchymal vessels (*arrow*, **A**).

C and **D,** 49-year-old man with prostate cancer. T2-weighted MR image (**C**) and corresponding photomicrograph (H and E, ×10) (**D**) show periglandular chronic inflammation along with intraluminal hemosiderin-laden macrophages (*arrow*, **C**).

E and **F,** 52-year-old man with prostate cancer. T2-weighted MR image (**E**) and corresponding photomicrograph (H and E, ×10) (**F**) show intraluminal acute inflammation with periglandular chronic inflammation (*arrow*, **E**).
G and **H,** 57-year-old man with prostate cancer. T2-weighted MR image (**G**) and corresponding photomicrograph (H and E, ×10) (**H**) show nonspecific atrophic glands (*arrow*, **G**).

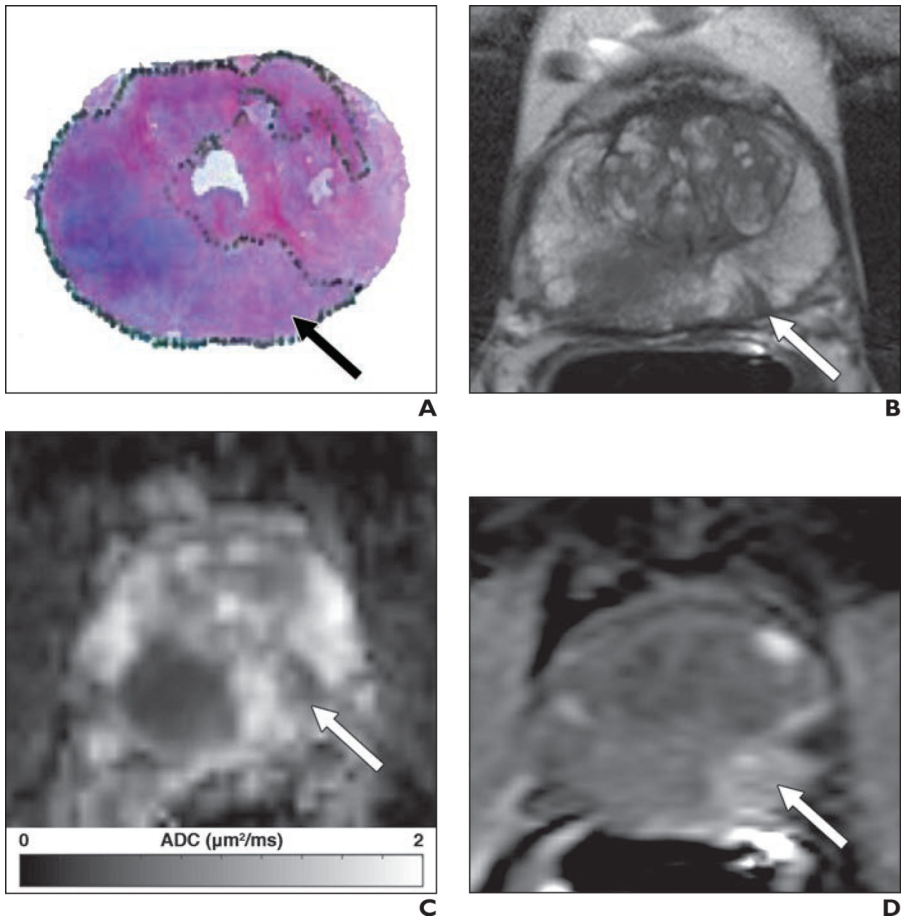

Fig. 2—.

62-year-old man with prostate-specific antigen level of 10.24 ng/mL.

A–D, H and E–stained whole mount histology section (**A**) and multiparametic MR images (**B** and **C**) show wedge-shaped lesion on T2-weighted image that was confirmed on histologic correlate as prostate cancer with Gleason score of 3 + 4. Apparent diffusion coefficient (ADC) map (**C**) shows wedge-shaped lesion as highly hypointense region. Dynamic contrast-enhanced (DCE) MRI (**D**) shows early enhancement of wedge-shaped lesion. Arrow (**A**–**D**) shows location of malignant wedge-shaped feature on T2-weighted MR image in left peripheral zone. Same cancer with Gleason score of 3 + 4 in right peripheral zone is clearly visible as hypointense region on T2-weighted MR image (**B**) and ADC map (**C**) but shows no early enhancement on DCE-MR image (**D**), which is clinically relevant finding.

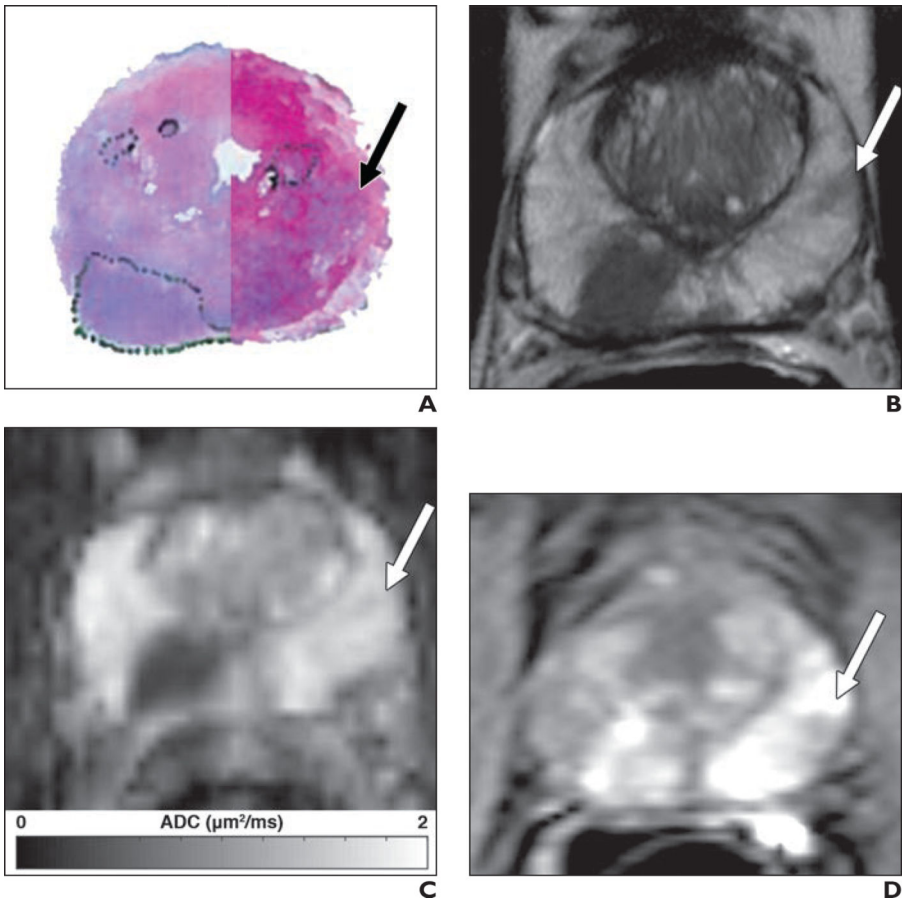

Fig. 3—.

62-year-old patient with prostate-specific antigen level of 10.2 ng/mL.

A–D, H and E–stained whole mount histology section (**A**) and multiparametic MR images (**B** and **C**) show wedge-shaped features of lesion on T2-weighted MR image (**B**) that was histologically confirmed as benign prostate tissue. Apparent diffusion coefficient map (**C**) shows lesion as isointense region, and dynamic contrast-enhanced (DCE) MRI (**D**) shows early enhancement of lesion. Arrow (**A**–**D**) shows location of benign wedge-shaped feature on T2-weighted MR image in left peripheral zone. Cancer with Gleason score of 3 + 4 in right posterior peripheral zone is clearly visible as hypointense region on T2-weighted MR image and ADC map (**B** and **C**) and shows early enhancement on DCE-MR image (**D**), which is clinically relevant finding.

TABLE 1:

MRI Parameters

Imaging Sequence	Pulse Sequence	FOV (mm^2)	Scan Matrix Size	In-Plane Resolution (mm)	TR/TE	Slice Thickness (mm)	Flip Angle (°)
Axial T2-weighted MRI	SE and TSE	160 × 160	400 × 400	0.4 × 0.4	8230/115	3	90
DWI[a]	SE EPI	180 × 180	120 × 120	1.5 × 1. 5	6093/80	3	90
DCE-MRI[b]	T1-weighted fast field-echo	250 × 385	200 × 308	1.25 × 1.25	4.8/2.8	3.5	10

Note—SE = spin echo, TSE = turbo spin echo, DCE = dynamic contrast-enhanced, EPI = echo-planar imaging.

[a]The b values used were 0, 50, 150, 990, and 1500 s/mm^2.

[b]The contrast agent gadobenate dimeglumine (MultiHance, Bracco) was injected at a rate of 2.0 mL/s and was followed by a 20-mL saline flush. The contrast dose (0.1 mmol/kg) was based on the patient's weight. DCE-MRI T1-weighted images were obtained with a temporal resolution of approximately 8.3 seconds at 60 dynamic scan points over 8.3 minutes.

AJR Am J Roentgenol. Author manuscript; available in PMC 2019 March 28.

Table 2:

Pathologic Outcome and Multiparametric MRI Features of Wedge-Shaped Prostate Lesions

Feature	Malignant Lesions (*n* = 12)	Benign Lesions (*n* = 23)
ADC map signal intensity		
Highly hypointense	10 (83)	7 (30)
Mildly hypointense	2 (17)	13 (57)
Isointense	0 (0)	3 (13)
DCE-MRI enhancement		
Early enhancement	7 (58)	8 (35)
No early enhancement	5 (42)	15 (65)
DCE-MRI curve type[a]		
Type 1 (progressive enhancement)	6 (50)	6 (26)
Type 2 (plateau)	2 (17)	10 (43)
Type 3 (wash-in and washout)	4 (33)	7 (30)

Note—Data are the number (%) of lesions. ADC = apparent diffusion coefficient, DCE = dynamic contrast-enhanced.

[a]Percentages for benign lesions do not total 100% because of rounding.